Publ. Astron. Obs. Belgrade No. 96 (2017), 71 - 78 *Invited Lecture*

COMPUTATION OF TRANSIT ORBITS IN THE THREE-BODY-PROBLEM WITH FAST LYAPUNOV INDICATORS

M. GUZZO[1] and E. LEGA[2]

[1] *Università degli Studi di Padova, Dipartimento di Matematica, Via Trieste, 63 - 35121 Padova, Italy*
E–mail: guzzo@math.unipd.it

[2] *Université de Nice Sophia Antipolis, CNRS UMR 7293, Observatoire de la Côte d'Azur, Bv. de l'Observatoire, C.S. 34229, 06304 Nice cedex 4, France*
E–mail: elena.lega@oca.eu

Abstract. We describe in this paper how to compute special orbits of the three-body-problem which transit from a region which is internal to the secondary mass to the region which is external to the binary system, by using a recent variant of the Fast Lyapunov Indicator method. The orbits are obtained by slightly changing the initial conditions of orbits which are heteroclinic to Lyapunov orbits of the Lagrangian equilibrium points L_1 and L_2 of the restricted three-body-problem.

1. INTRODUCTION

The orbits of gravitational systems may be very complicated, due to resonances and close encounters with massive bodies. An important example is represented by the dynamics of particles which pass close to the so-called Lagrangian collinear equilibrium points L_1, L_2, L_3 of the three-body-problem. The importance of the dynamics near the Lagrangian collinear equilibria, especially L_1 and L_2, has been extensively discussed in the last years in connection with space-mission design for several reasons (see, for example, the review paper by Belló et al. 2010, and references therein). On the one hand, the collinear equilibria of the Earth-Moon and of the Sun-Earth systems, and the associated Lyapunov periodic orbits, may be considered as interesting orbits where to place spacecrafts; on the other hand, orbits transiting from the region which is internal to the region which is external to a binary system, with the lowest possible energies, are interesting for example for explaining the dynamics of some Jupiter-family comets (see Ross 2004) or that of Earth's Minimoons (Bolin et al. 2014). These orbits are constructed from the special dynamics which occur in the neighborhoods of L_1 and L_2 and are difficult to compute, since chaos dominates their dynamics: very small changes of the initial conditions may produce orbits which are qualitatively very different. In this context, numerical integrations of individual orbits are not very meaningful, since from the numerical integration of one or a few orbits it is difficult to understand how these orbits behave with small changes of the initial

conditions, or of the model. After the first numerical detection of chaotic motions in Hénon and Heiles 1964, many methods of investigations of chaotic dynamics, based on numerical computations of large sets of initial conditions, have been developed. In particular, the topic had a certain relevance in celestial mechanics, where many examples of chaotic diffusion and chaotic transport related to resonances in the Solar System had been reported (see, for example, Laskar 1990, Milani et al. 1997, Murray et al. 1998, Morbidelli and Nesvorný 1999). In the last decade, many methods of numerical detection of the chaos related to resonances have been developed on the base of extensive computations of dynamical indicators on grids of initial conditions of the phase–space. These methods are essentially based on the computation of indicators derived from Fourier analysis–such as the frequency analysis (see Laskar 1990, 1993)– or on some indicators derived from the theory of Lyapunov exponents, such as the Fast Lyapunov Indicator (FLI hereafter) introduced in Froeschlé et al. 1997 (for applications of these methods see Robutel and Galern 2006, Guzzo 2005, 2006, Wayne et al. 2010, Guzzo et al. 2002). This paper is concerned with an application of the Fast Lyapunov Indicator, whose ability of detection of chaotic diffusion has been extensively studied in Lega et al 2003, Guzzo et al. 2005, 2011, Froeschlé et al 2000, 2005, Todorović et al 2011. More recently, the FLI has been used for a different purpose, that is for the computation of certain surfaces of the phase–space, the so called stable and unstable manifolds, whose structure is fundamental to understand the dynamics of a chaotic system (see Villac 2008, Guzzo 2010, Guzzo et al. 2009, Lega et al. 2010, Guzzo and Lega 2013). In particular, in the three-body-problem these surfaces are called the 'tube' manifolds, and are defined by all the initial conditions of the phase–space whose orbits are asymptotic (in the past-for the unstable manifold- or in the future-for the stable manifold) to a Lyapunov periodic orbit of L_1 and L_2. These structures provide all important information related to the transit orbits (see, for example, Koon et al. 2008). Many methods of detection of the stable/unstable manifolds have been developed in the literature (see, for example, Simó 1989, Krauskopf B. and Osinga 2003), essentially based on extremely precise preliminary local approximations of the manifolds, combined with some advancing front technique of surfaces' reconstruction. We present here a computation of the tube manifolds of the restricted three-body-problem recently obtained in Guzzo and Lega 2014, based on a modification of the traditional FLI. On the base of these computations, we produce, as an example, a peculiar orbit of the Sun-Jupiter three-body-problem which transits from the region which is internal to the orbit of Jupiter to the region which is external to the Sun-Jupiter system, and in particular the transit occurs after some librations around L_1 and L_2 and a close encounter with Jupiter.

The paper is structured as follows. In Section 2 we review the properties of the dynamics near the Lagrangian equilibrium points L_1, L_2, and the definition of the tube manifolds. In Section 3 we report the computations obtained with the modified Fast Lyapunov Indicators. Finally, in Section 4 we provide conclusions.

2. THE TUBE MANIFOLDS OF THE THREE-BODY-PROBLEM

In its simplest formulation, i.e. the planar circular restricted three-body-problem, the problem is defined by the motion of a massless body P in the gravitation field of two massive bodies P_1, P_2, called primary and secondary bodies respectively, which

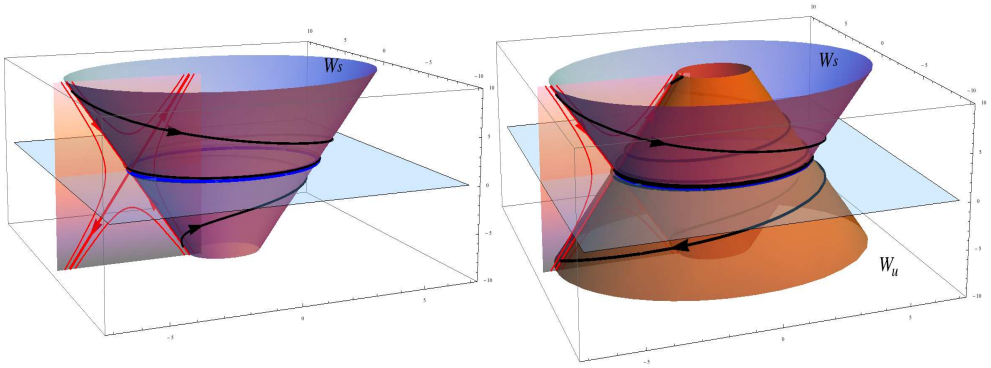

Figure 1: Sketch of the dynamics near a Lyapunov orbit, represented as the blue curve. In any section transverse to the orbits the dynamics is characterized by a curve of initial conditions which converge to the periodic orbit for positive times and a curve of initial conditions which converge to the periodic orbit for negative times; while converging to LL_1 (or LL_2), the orbits turn around the periodic orbit, so that there exist two surfaces, which topologically are cylinders, of orbits which converge to the periodic orbit for positive times (violet surfaces in the left panel) and also two surfaces of of orbits which converge to the periodic orbit for negative times (the additional surfaces in the right panel). These cylinders are the stable and unstable manifolds of LL_1 (or LL_2) respectively, that is the tube manifolds.

orbit uniformly around their common center of mass. In a rotating frame xOy, the equations of motion of P are:

$$\begin{cases} \ddot{x} &= 2\dot{y} + x - (1-\mu)\frac{x+\mu}{r_1^3} - \mu\frac{x-1+\mu}{r_2^3} \\ \ddot{y} &= -2\dot{x} + y - (1-\mu)\frac{y}{r_1^3} - \mu\frac{y}{r_2^3} \end{cases} \tag{1}$$

where the masses of P_1 and P_2 are $1-\mu$ and μ respectively; their coordinates are $(-\mu, 0)$ and $(1-\mu, 0)$; their revolution period is 2π and: $r_1^2 = (x+\mu)^2 + y^2$, $r_2^2 = (x-1+\mu)^2 + y^2$. As it is well known, equations (1) have a constant of motion, the so–called Jacobi constant which we denote by $\mathcal{C}(x, y, \dot{x}, \dot{y})$, and five equilibria denoted by $L_1, \ldots, L_5$. The equilibrium L_2 is particularly important to study the dynamics of the orbits which transit from the region which is internal (external) to the orbit of the secondary mass to the region which is external (internal) to the binary system. In fact, these transits are in principle possible only for the orbits with values $\mathcal{C}_*$ of the Jacobi constant strictly smaller than the value $\mathcal{C}_2 = \mathcal{C}(x_{L_2}, 0, 0, 0)$ at L_2. Moreover, for $\mathcal{C}_* < \mathcal{C}_2$ close to $\mathcal{C}_2$, two periodic orbits around the equilibria L_1 and L_2 exist: the so called Lyapunov orbits of L_1, L_2, which will be hereafter denoted by LL_1, LL_2. Also, the region of the orbit plane x, y which can be visited by orbits with Jacobi constant $\mathcal{C}_*$ has the peculiar shape of a bottle-neck, and LL_1, LL_2 are located at the entry and exit of the bottle-neck. The orbits LL_1, LL_2 are normally hyperbolic: in

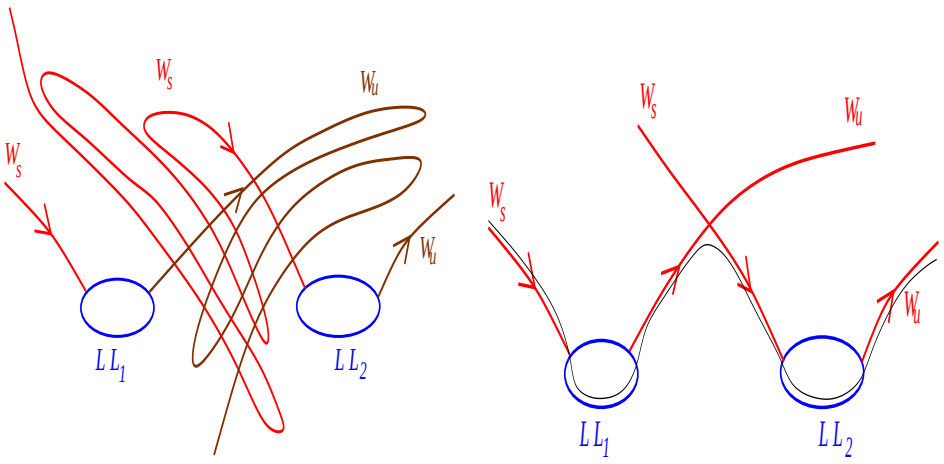

Figure 2: On the left panel we symbolically sketch the possible complicated structure of the stable and unstable manifolds of LL_1, LL_2. In particular, many intersections exist. Any intersection point (such as the one symbolically represented in the right panel) belongs to a heteroclinic orbit, which is asymptotic in the past to LL_1, and in the future to LL_2. With a suitable small variation of the initial conditions, we obtain a transit orbit, such as the black curve symbolically represented in the right panel.

any section transverse to the orbits the dynamics is characterized by a curve of initial conditions which converge to the periodic orbit for positive times and a curve of initial conditions which converge to the periodic orbit for negative times (see Figure 1-left panel); while converging to LL_1 (or LL_2), the orbits turn around the periodic orbit, so that there exist two surfaces, which topologically are cylinders, of orbits which converge to the periodic orbit for positive times and two surfaces of orbits which converge to the periodic orbit for negative times. These cylinders are the stable and unstable manifolds of LL_1 (or LL_2) respectively, that is the so called 'tube' manifolds.

3. COMPUTATION OF THE TUBE MANIFOLDS AND TRANSIT ORBITS WITH FAST LYAPUNOV INDICATORS

Stable and unstable manifolds in non-integrable systems usually have a complicated topology, characterized by many typical lobes (see Figure 2); this is also the case of the tube manifolds of the three-body-problem. Analytic methods allows us to compute only the local part of the manifolds, close to the Lyapunov orbits. To extend the knowledge of the manifolds beyond the local part we need to use numerical methods. In order to study the transit orbits we are interested, in particular, in the computation of the intersections between the unstable manifold of LL_1 with the stable manifold of LL_2. An initial condition in these intersections belongs to a so called heteroclinic orbit (see Figure 2), that is an orbit which is asymptotic in the past to LL_1, and in the future to LL_2. A recent variant of the FLI, specifically introduced in Guzzo and Lega 2014 for the detection of the stable or unstable manifolds of selected periodic orbits, allows to detect the heteroclinic intersections of different manifolds. The new indicator is defined as follows. Let us consider a system of first order differential

equations $\dot{x} = F(x)$, $x \in \mathbb{R}^n$, and a normally hyperbolic periodic orbit γ. The new indicator is defined with reference to some smooth window function $u(x) \geq 0$ such that $u(x) \sim 1$ close to γ, and $u(x) = 0$ for x distant from γ more than some threshold ρ (there is a certain freedom of choice of ρ; see Guzzo and Lega 2014, and below, for technical details). Then, for any phase–space initial condition $x(0)$ and any initial vector $v(0) \in \mathbb{R}^n$ we denote by $x(t)$ the solution of the differential equations with initial condition $x(0)$ and by $v(t)$ the solution of the variational equations: $\dot{v} = \left(\frac{\partial F}{\partial x}(x(t))\right) v$. The Fast Lyapunov Indicator of $x(0)$ modified with the window functions $u(x)$, at time T is defined by:

$$FLI_u(x(0), v(0), T) = \int_0^T u(x(t)) \frac{v(t) \cdot \dot{v}(t)}{\|v(t)\|^2} dt. \tag{2}$$

For any selected periodic orbit γ, with a careful choice of the window function $u(x)$ and of the total integration time T, the FLI indicator (2) detects the stable manifold of γ if $T > 0$ (the unstable manifold if $T < 0$) with very high precision: as it is proved in Guzzo and Lega 2014, the modified FLI has its highest values on the points of the manifolds, and rapidly decays outside the manifold.

For the computation of the tube manifolds of LL_1, LL_2, we define the equations of motion of the three-body-problem, and its variational equations, in the space of the variables obtained by regularizing equations (1) with respect to the secondary mass, as in Lega et al. 2011, Guzzo and Lega 2013; we use the window function

$$u(x) = \begin{cases} 1 & \text{if} \quad |x - \gamma| \leq \frac{r}{2} \\ \frac{1}{2}[\cos((\frac{|x-\gamma|}{r} - \frac{1}{2})\pi) + 1] & \text{if} \quad \frac{r}{2} < |x - \gamma| \leq \frac{3r}{2} \\ 0 & \text{if} \quad |x - \gamma| > \frac{3r}{2} \end{cases} \tag{3}$$

where r is a parameter, and $|x - \gamma|$ denotes the distance between x and γ. Then, we obtained sharp representations of the intersections between the unstable manifold of LL_1 and the stable manifold of LL_2 with the two–dimensional surface of the space of the Cartesian coordinates and velocities $x, y, \dot{x}, \dot{y}$:

$$\Sigma = \{(x, y, \dot{x}, \dot{y}) : \quad y = 0 \quad , \quad \dot{y} \geq 0 : \quad \mathcal{C}(x, 0, \dot{x}, \dot{y}) = \mathcal{C}_*\} \tag{4}$$

by computing the modified FLI defined in (2) on a refined grid of initial conditions on Σ using the same initial tangent vector $v(0)$, a negative time $-T_1$ and $r = 10^{-3}$ for the unstable manifold of LL_1, and a positive time T_2 and $r = 5\ 10^{-4}$ for the stable manifold of LL_2. In such a way, for any $x, \dot{x}$ we obtained two modified FLIs, which we denote by FLI_1, FLI_2. Then, we represented on the same picture, for any initial condition $x, \dot{x}$, a weighted average of the two indicators:

$$\frac{w\ \mathrm{FLI}_1 + \mathrm{FLI}_2}{(w + 1)}, \tag{5}$$

for a convenient choice of $w > 0$. The results are represented in Figure 3: the stable and unstable manifolds appear on the picture as the curves characterized by the highest values of the indicator, as it is expected from the theory.

We clearly appreciate different lobes of both manifolds, as well as many intersection points, providing heteroclinic orbits. The FLI computation can be repeated by

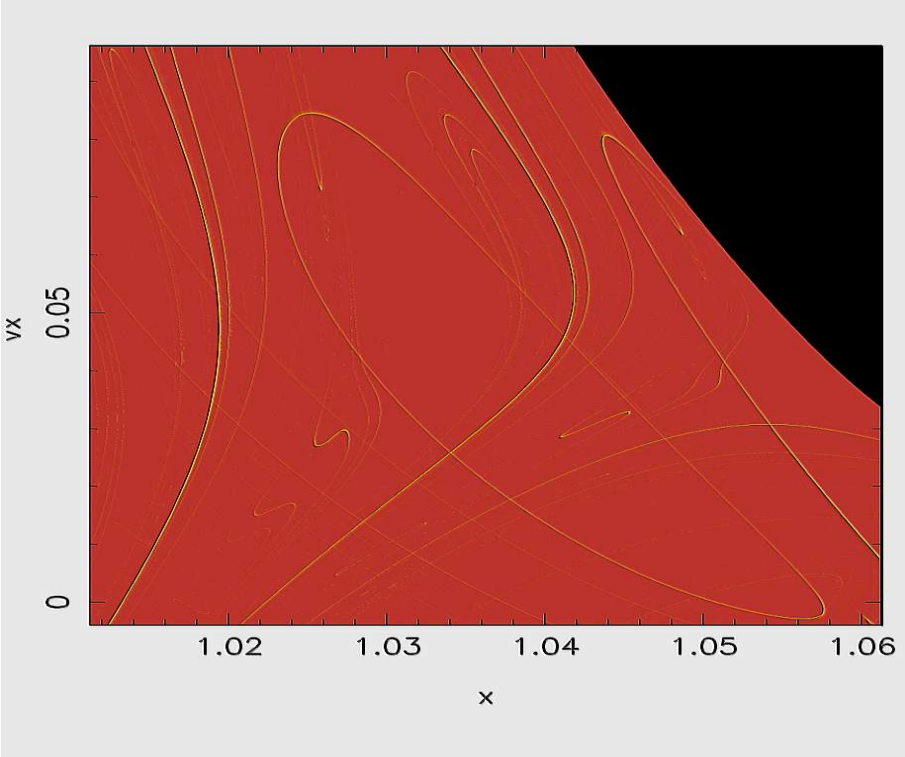

Figure 3: FLI computation of the unstable manifold of LL_1 and the stable manifold of LL_2 for the Sun-Jupiter systems and $\mathcal{C}_*$ slightly smaller than $\mathcal{C}_2$. The panel represents the values of the modified FLIs (5) computed on the section Σ: on each point $x, \dot{x} = vx$ of the panel we represent its FLI value with a color scale, so that the unstable manifold of LL_1 and the stable manifold of LL_2 appear as the yellow curves. The different lobes of the manifolds are clearly visible on this picture (obtained with $T_1 = T_2 = 5$) as well as many intersection points, which are the heteroclinic points described in the text. The figure, first obtained in Guzzo and Lega 2014, has been here represented with some graphic filter in order to appreciate more clearly the manifolds.

zooming close to an intersection point, in order to detect the heteroclinic points with all the desired precision, such as in Figure 4: the heteroclinic point is obtained with 15 digits of precision. In Figure 5, left panel, we report the orbit corresponding to this heteroclinic point. Since the heteroclinic orbit transit from LL_1 and LL_2, with a very small variations of its initial conditions we easily obtain the transit orbit reported in Figure 5, right panel.

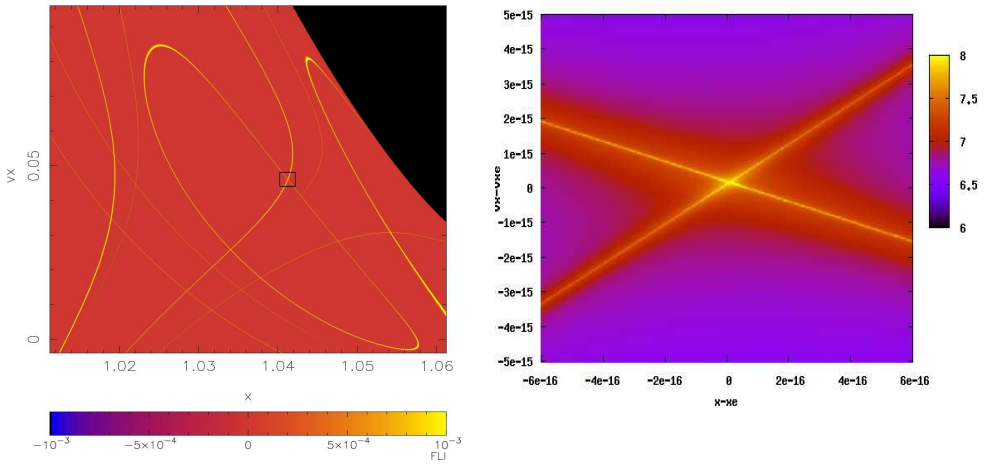

Figure 4: On the left panel (see Fig. 3) we select an heteroclinic point, in the box. On the right panel we zoom very close to it (set as the origin of the picture), so that we determine the heteroclinic intersection with 15 digits of precision. Both figures had been published in Guzzo and Lega 2014: *Copyright 2014 Society for Industrial and Applied Mathematics. Reprinted with permission. All rights reserved.*

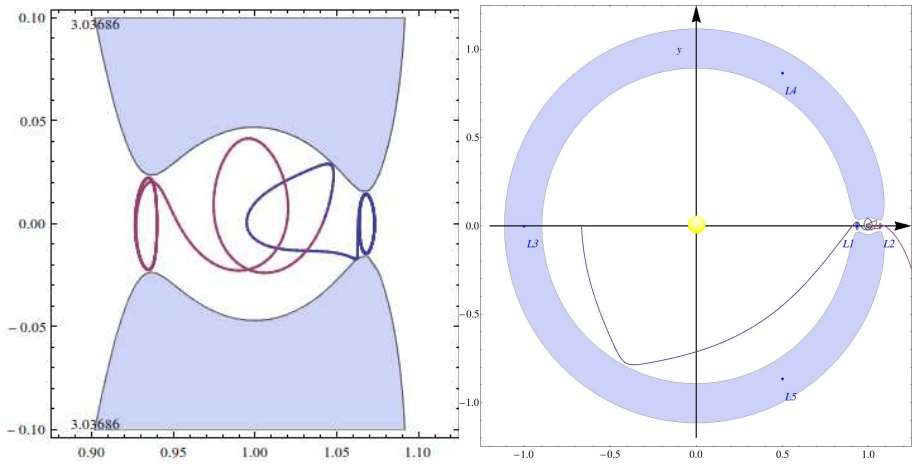

Figure 5: In the left panel we report the projection on the plane (x, y) of the heteroclinic orbit found with the FLI computation of Figure 4. The shaded area represents the region where orbits with Jacobi constant equal to $\mathcal{C}_*$ cannot enter. With a very small correction to the initial conditions of this orbit, we obtain the transit orbit reported in the right panel. The figure in the left panel had been published in Guzzo and Lega 2014: *Copyright 2014 Society for Industrial and Applied Mathematics. Reprinted with permission. All rights reserved.*

4. CONCLUSIONS

The modified FLI indicator introduced in Guzzo and Lega 2014 has been used to compute the heteroclinic intersections of different stable and unstable manifolds of the three-body-problem, and thus transit orbits. Since the application of the method is robust by considering more complicated dynamical models, we expect that it can be used to compute transit orbits in realistic models of the Solar System.

References

Belló, M., Gómez, G. and Masdemont, J.: 2010, in *Space Manifolds Dynamics: Novel Spaceways for Science and Exploration"*, proceedings of: "Novel spaceways for scientific and exploration missions, a dynamical systems approach to affordable and sustainable space applications", Avezzano, 15-17 October 2007. Editors: Perozzi and Ferraz Mello. Springer.

Bolin, B., Jedicke, R., Granvik, M., Brown, P., Howell, E., Nolan, M. C., Jenniskens, P., Chyba, M., Patterson, G., Wainscoat, R.: 2014, *Icarus*, **241**, 280-297.

Froeschlé, C., Guzzo, M. and Lega, E.: 2000, *Science*, **289**, n. 5487, pp. 2108-2110.

Froeschlé, C., Guzzo, M. and Lega, E.: 2005, *Cel. Mech. and Dyn. Astron.*, **92**, 1-3, pp. 243-255.

Froeschlé, C., Lega, E. and Gonczi, R.: 1997, *Celest. Mech. and Dynam. Astron.*, **67**, pp. 41-62.

Guzzo M., Kenežević, Z. and Milani, A.: 2002, *Cel. Mech. Dyn. Astr.*, **83**, pp 121140.

Guzzo, M.: 2005, *Icarus*, **174**, n. 1., pp. 273-284.

Guzzo, M.: 2006, *Icarus*, **181**, pp. 475-485.

Guzzo, M.: 2010, in *Space Manifolds Dynamics: Novel Spaceways for Science and Exploration"*, proceedings of the conference: "Novel spaceways for scientific and exploration missions, a dynamical systems approach to affordable and sustainable space applications" held in Avezzano, 15-17 October 2007. Editors: Perozzi and Ferraz Mello. Springer.

Guzzo, M., Lega, E. and Froeschlé, C.: 2005, *DCDS B*, **5**, 3, pp. 687-698.

Guzzo, M., Lega, E. and Froeschlé, C.: 2009, *Physica D*, **182**, pp. 1797–1807.

Guzzo, M., Lega, E. and Froeschlé, C.: 2011, *Chaos*, **21**, 3.

Guzzo, M. and Lega, E.: 2013, *Monthly Notices of the Royal Astronomical Society*, **428**, 2688-2694.

Guzzo, M. and Lega, E.: 2013, *Chaos*, **23**, n. 023124.

Guzzo, M. and Lega, E.: 2014, *SIAM J. APPL. MATH.*, **74**, No. 4, pp. 1058-1086.

Hénon, M. and Heiles, C.: 1964, *The Astronomical Journal*, **69**, pp. 73-79.

Koon, W. S., Lo, M. W., Marsden, J. E. and Ross, S. D.: 2008, Dynamical Systems, the three body problem and space mission design. Marsden Books. ISBN 978-0-615-24095-4.

Krauskopf, B. and Osinga, H. M.: 2003, *SIAM J. Appl. Dyn. Syst.*, **2**, 4, 546-569.

Laskar, J.: 1990, *Icarus*, **88**, pp. 266-291.

Laskar, J.: 1993, *Physica D*, **67**, pp. 257-281.

Lega, E., Guzzo, M. and Froeschlé, C.: 2003, *Physica D*, **182**, pp. 179-187.

Lega, E., Guzzo, M. and Froeschlé, C.: 2010, *Cel. Mech. and Dyn. Astron.*, **107**, p. 115-127.

Lega, E., Guzzo, M. and Froeschlé, C.: 2011, *MNRAS*, **418**, pp. 107-113.

Milani, A., Nobili, A. M. and Knezevic, Z.: 1997, *Icarus*, **125**, 1, pp. 13-31.

Morbidelli, A. and Nesvorný, D.: 1999, *Icarus*, **139**, 2, p. 295-308.

Murray, N., Holman, M. and Potter, M.: 1998, *AJ*, **116**, 5, p. 2583-2589.

Robutel, P. and Galern, F.: 2006, *Monthly Notices of the Royal Astronomical Society*, 372.

Ross, S. D.: 2004, *Cylindrical Manifolds and Tubes Dynamics in the Restricted Three-Body Problem (Ross Thesis)*, California Institute of Technnology, Pasadena.

Simó, C.: 1989, in *Modern Methods in Celestial Mechanics*, D. Benest, Cl. Froeschle, eds, Gif-sur-Yvette: Editions Frontières, p. 285-329.

Villac, B. F.: 2008, *Cel. Mech. and Dyn. Astron.*, 102, pp. 29-48.

Todorović, N., Guzzo, M., Lega, E. and Froeschl'e, C.: 2011, *Cel. Mech. and Dyn. Astron.*, **110**, 389-398.

Wayne, B. H., Malykh, A. V. and Danforth, C. M.: 2010, *MNRAS*, **407**, 3, pp. 1859-1865.